Synthesis of new Semi Nucleoside from Indole and Investigation Biological activity and its effect on DNA.

Khattab OmarAzeez[1], Ibtihal QahtanAbdalluh[1], Hala M.G. Al-Zahawi[2]
Email: Khattabomer7@gmail.com
[1]Chemistry Department, College of Science, University of TiKrit, Iraq
[2]Chemistry Department, College of Science, University of Kirkuk, Iraq

Abstract

This study focused on the widely used indole derivatives in medical fields, which were prepared by substitution reaction on the C3 position, then protecting the position 1 by a good leaving group until it is replaced with a pentacyclic sugar such as the compound KI3, KI5, KI10, and identification of these aforementioned compounds by HNMR and IR spectra. The inhibition zone was studied against positive and negative bacteria, fungi and the effect of their binding with DNA.

Keywords: semi nucleoside, bioactivity, binding.

1. Introduction

Indoles and its derivatives have occupied a unique place in the chemistry of nitrogen heterocyclic compounds in figure1, because of their varied biological properties. But earlier derivatives of indoles were known for their dyeing properties. Only after the twentieth century, a large number of naturally occurring compounds like alkaloids [1], were known to possess indole nucleus. During this period the recognization of plant growth hormone heteroauxin and the essential amino acid tryptophan as the derivatives of indole have been added stimulus to the research. It is evident from literature that indole containing synthetic compounds and their derivatives are known to be associated with broad spectrum of biological activity like antipyretic activity, analgesic effect [2] anticonvulsant activity [3], few compounds were also reported as psychotropic agents, MAO inhibitors [4]. Nucleosides are a great family of natural compounds and their chemically modified analogs, which are characterized by great structural diversity. It's were the main constituents of DNA and RNA, respectively.

For a long period of time, nucleosides and nucleotides have been of great interest in their use as antivirals and antiparasitics [5, 6]. For example muraymycin nucleoside analogues successes in using these natural product nucleoside analogues for antibacterial therapies [7]. The innovative fleximers have shown potent activity against two coronaviruses - SARS and MERS [8], as well as filoviruses such as Ebola, Sudan and Marburg [9]. Expanding on those results, a focused structure activity relationship study to improve upon the anti-Ebola activity previously noted is reported in this issue. Binding of toxic ligands to DNA could result in undesirable biological processes, such as carcinogenesis or mutagenesis, from the thermodynamic information values published before Tanveer A. Wania ,et al show that hydrogen bonding is the main force involved in binding of ABR with ctDNA [10] .

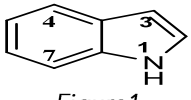

Figure1

In recent years the studying of interaction of small molecules with DNA has been much interest due to their potential candidature as therapeutic agents against a number of diseases [11]. DNA is the pharmacological target of many drugs that are currently in clinical use or in advanced clinical trials. Many clinically useful compounds against diseases such as cancer are known to exert their primary biological effects by modulating transcription or by interfering with replication [12]. Studying the interaction of small molecules with DNA is of current interest and

Has high significance. It provides assistance in the development of therapeutic drugs that may control the gene expression. New and more effective drugs can be designed which can recognize a specific site or conformation of DNA [13] .Three different noncovalent modes through which small molecules interact with DNA are electrostatic interactions, intercalative binding and groove binding. Electrostatic binding occurs due to the interaction between the negatively charged DNA phosphate backbone and the positively charged end of small molecules while intercalative binding occurs when small molecules intercalate within stacked base pairs thereby distorting the DNA backbone conformation [14] .Groove binding occurs due to hydrogen bonding or van der Waals interaction with nucleic acid bases and small molecules in the deep major groove or the shallow minor groove without causing any major distortion of the DNA backbone [15]. The availability of the genome sequence, the well-studied three-dimensional structure of DNA and the predictability of their accessible chemical and functional groups make DNA an attractive drug target. However, the number of known drugs targeting DNA is still very limited compared to the drugs targeting proteins [16].

2. Materials and Methods

The practical part includes the manufacture of a semi-nucleoside from indole and then the preparation of the stock solution.

Preparation of 3-(prop-2-yn-1-yl)-1H-indole: KI 3

doi.org/10.31838/hiv22.02.260 Received: 23.05.22, Revised: 24.06.22, Accepted: 01.08.22

The general method involved the installation of a terminal alkyne at the 3-position of indole via a zinc-mediated Barbier reaction [17, 18] ,which entailed treatment of indole with propargyl bromide and zinc dust in THF at ambient temperature to deliver 3-propargylindole in 30% yield.(0.62g) as shown in the scheme 1

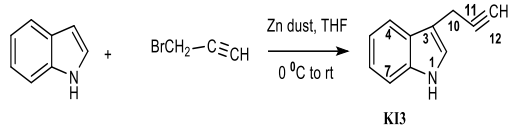

Scheme 1

Preparation of 4-(4-(1H-indol-3-yl) but-2-yn-1-yl) morpholine KI 5 [19, 20]

Added to the mixture of 3-(prop-2-yn-1-yl)-1H-indole (0.0129mol) and 20 ml of glacial acetic acid (0.0129 mol (0.474ml) of foraldehyde. The mixture is cooled to a temperature of 5 °C, then morpholine (0.0.0129 mol) (1.122ml) was added to the mixture. The solution was heated under reflux in water bath for 12hr,85-95C0 and stirred at room temperature for 24hr. 10% NaOH was added to the reaction mixture, the precipitate is separated by filter paper Recrystallized by ethyleacetate and Ethanol gave pure product. TLC was used to check the reaction result and purity of product by using mixture of Benzene: Ether (1:1). Also column chromatography was used to get ultrapure yield by using same mixture as mobile phase and silica gel (220-240 mesh) as stationary phase. (1.5g)

As shown in the scheme 2

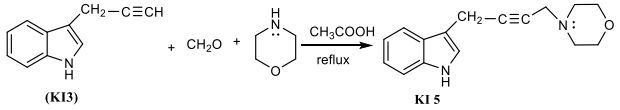

Scheme 2

Synthesis of compound (KI 10)

The compound KI10 is manufactured in three basic stages, firstly inserting a protection group to the position in which nitrogen is present, the second stage being the presence of a protected sugar containing a good leaving group to obtain a protected compound with a benzoyl group, and finally carrying out the hydrolysis process to produce a semi-nucleoside compound KI10 as shown in the following scheme 4 Below are mentioned these stages.

Synthesis of (3-(4-morpholinobut-2-yn-1-yl)-1H-indol-1-yl)

Mercury (II) chloride

5 mmol (1.27 g) of (4-(4-(1H-indol-3-yl) but-2-yn-1-yl) morpholine) (KI 5) is dissolved in hot distilled water, then (2 mmol) (0.08 g) of sodium hydroxide dissolved in (10 ml) of hot distilled water is added to it. Mercuric chloride (2.6 mmol) (0.71 g) of dissolved in (10 ml) hot distilled water, to which (10 ml) absolute ethanol is added to the mixture, and the mixture is reacted in a water bath (60-65) ° C for 2 hours, then filtered, the precipitate is washed with ethanol and crystallized.

Synthesis of 1-(1',3',4',6'-tetra-O-benzol-β-D-

Fructofuranosyl-3- propargylmethylmorpholineindol

Added (40 ml) of toluene to (2.1 moll) (1.4 g) of (1', 3', 4', 6'- tetra-O-benzoyl-β-D-fructofuranose) in the presence of a boiling stone, (2.1 mmol) (0.1 g) of (3-(4-morpholinobut-2-yn-1-yl)-1H-indol-1- yl) mercury (II) chloride) added to the mixture. At (130-1350C) refluxed with stirring the mixture for 3.5hr and then filtrate, washed by CHCl3and crystallized. A residue was obtained as red crystal (0.43g) (27%yield). IR (film), 1425 cm-1 of (C-N).

Synthesis of 1-(1', 3', 4', 6'-tetra-hydroxy-β-

D-fructofuranosyl-3 Propargylmethylmorpholineindol (KI 10)

(1g,1.3mmol)1-(1',3',4',6'-tetra-O-benzol-β-D-Fructofuranosyl-3- propargylmethylmorpholineindol in (45ml) ethanol absolute with (2-3)

Drops of 36%HCl. The mixture was refluxed with stirring for 1.5 hrand evaporated to dryness to give a white powder (0.36g, 72%). IR (KBr disc), 3371cm-1 brod signal of (OH).

Preparation stock solution of CT-DNA

Stock solution of DNA was prepared by dissolving 10 mg of calf-thymus DNA per milliliter of 10 mM Tris–HCl buffer (pH 7.4). The stock solution was kept at 8 C for 24 h and stirred occasionally for complete homogenization.

Final concentration of the stock CT-DNA solution was measured spectrophotometrically using excitation coefficient of 6600 cm-1 [21]. The UV absorbance of 250 time's diluted CT-DNA solution was found 0.740 at 260 nm with a path length of 1 cm. The final concentration of CT-DNA stock solution was 28 mM (molarity of phosphate group) [22].

Preparation stock solution of Idole derivatives [KI1]

The indole derivatives [KI10] solution was prepared in ultra-pure water and incubated for 96 h for complete hydrolysis. A series of solutions with varying concentrations of [KI10] were prepared. [KI10] solutions of different concentration so prepared were added drop wise to CT-DNA solutions.

The [KI1]/CTDNA ratios (r) were kept 1/100, 1/50, 1/20, 1/10 and 1/5. The final concentration of the DNA was 14 mM in all the solutions used for infrared measurement [22].

3. Result and Conclusion

Identification of compound KI3

Derivative were prepared by the reaction between indole and propargyle bromide and zinc dust in THF at ambient temperature. The ratio was 1:1:1 for each one of them. Snyder et al. [23] The synthesized derivative KI3 were characterized by measuring melting points, color change, TLC, FT-IR (FT-IR Shimadzu Fourier Transform Infrared Spectrophotometer 8400 S (KBr)) and 1H-NMR technique (Proton Nuclear Magnetic Resonance Spectroscopy – Bruker Ultra shield 400 MHZ – By using (TMS) as reference and (DMSO d6) as solvent). The spectrum IR for compound KI3 showed in table (1) bands (N-H)str peaks appeared of indole in (3431 cm-1) ,bands appeared in (2123Cm-1) back to triple bond (C≡C) of alkyne, bands absorption at (3300Cm-1) for terminal hydrogen of alkyne group ,bands absorption at (3041 cm-1) appeared back to (C-H)str aromatic, (2907.32cm-1) for (C-H)str aliphatic, bands absorption appearance for (C-N) at (1458.30cm-1) and at (1618.33Cm-1) for (C=C) aromatic.

The spectrum H1NMR for compound KI3 showed in table (2) singlet signal at (δ, 2.5ppm) due to protons of the solvent

(DMSO), three singlet signal at (δ, 2.08ppm) for CH of alkyne group in position C12, the second singlet signal at (δ,3.36ppm) for CH2 in position C11and the last one at (δ,10.73ppm)for NH in N1, the spectrum appeared triplet signals at (δ,6.66ppm)for CH in C5, at (δ,7.24ppm) for CH in C6,the spectrum showed doublet signal at (δ,6.88ppm) for CH in C7,at (δ,7.26ppm) for CH in C4. All the values we are corresponding to literatures [17, 24].

Table (1) shows the FT-IR values for synthesized derivative (KI3)

Comp. NO.	Structure	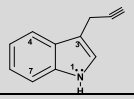 IR υ cm-1 (KBr)					
		N-H	C-H Aliph	C-H Ar.	C=C Ar.	C-N	others
KI3 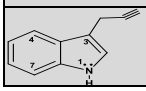		3431	2907	3041	1618	1458	2123(C≡C) 3300 C≡C-H

Table (2) The spectrum H1NMR for compound KI3

Comp. No	Structure	Chemical Shift ppm	Type of signal	Position of H
KI3	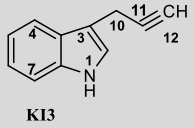 KI3	2.49 CH3	S	DMSO
		2.08 CH	S	C12
		3.36 CH2	S	C10
		7.24 CH	S	C2
		10.73 NH	S	N1
		7.14 CH	d	C7
		6.88 CH	t	C6
		6.66 CH	t	C5
		7.12 CH	d	C4
s = singlet, d=doublet, t= triplet, m= multiplet				

Identification of KI5 Derived from KI3 by formaldehyde

Derivative (15) were prepared by the reaction between (14), secondary amines and formaldehyde. The ratio was 1:1:1 for each one of them in (5-15) ml acetic acide as a solvent. The general equation of preparation appears below scheme 3 [23].

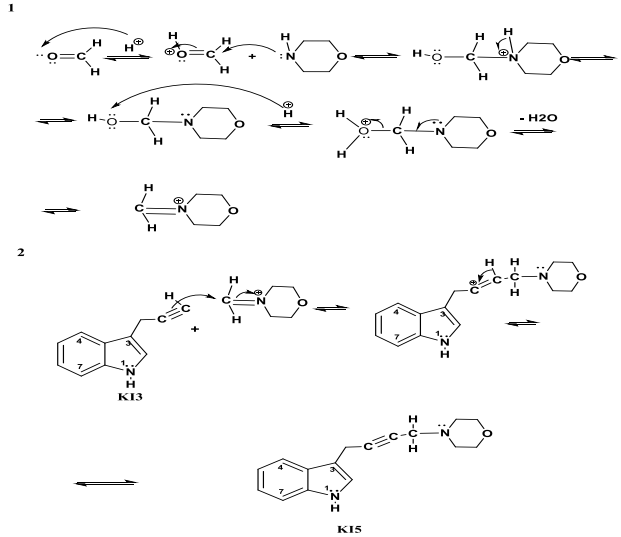

Scheme (3) Mechanism of synthesis compound KI5 from KI3

The synthesized derivative KI5 were characterized by measuring melting points, color change,TLC, FT-IR, and 1H-NMR technique. The spectrum IR for compound KI5 showed in table (3) bands (N-H)str peaks appeared of indole in (3431 cm-1) ,bands appeared in (2063Cm-1) back to triple bond (C≡C) of alkyne, bands absorption at (3300Cm-1) for terminal hydrogen of alkyne group, was disappeared, bands absorption at (3068 cm-1) appeared back to (C-H)str aromatic, the spectrum showed band shifted from (2907.32cm-1) to (2978 cm-1) for (C-H)str aliphatic, bands absorption appearance for (C-N) at (1425.44 cm-1) and at (1618.33Cm-1) for (C=C) aromatic was shifted to(1681.98 cm-1) . The spectrum H1NMR for compound KI5 showed in table(4), multiplet signal at (δ,2.06-2.07ppm) for CH2 of morpholine in position C14,C15,C16,C17, two singlet signal appeared at (δ,3.51ppm) for CH2 in C10and C13,multiplet signal appeared at(δ,7.91 – 8.19 ppm) for five aromatic protons, too the spectrum showed singlet signal shifted from (δ,10.97 ppm) to (δ,13.29 ppm) hiperconjocated of secondary amine morpholine. All the values we are corresponding to literatures [17, 24].

Table (3) shows the FT-IR values for synthesized derivative KI5.

Comp. NO.	Structure	IR υ cm-1 (KBr)					
		N-H	C-H Aliph	C-H Ar.	C=C Ar.	C-N	others
KI5	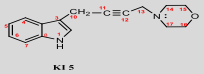 KI5	3431	2978	3068	1681	1425	2063 C≡C

Table (4) The spectrum H1NMR for compound KI5				
Comp. No	**Structure**	**Chemical Shift ppm**	**Type of signal**	**Position of H**
KI5	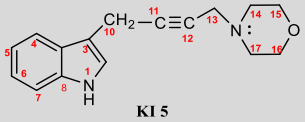 KI 5	2.5 CH3	S	DMSO
		2.07 CH2 2.06 CH2	M m	C14,C17 C15,C16,
		3.51 CH2	S	C10,C13
		13.29 NH	S	N1
		7.91-8.19 CH	m	C2,C4,C5,C6,C7
s = singlet, d=doublet, t= triplet, m= multiplet				

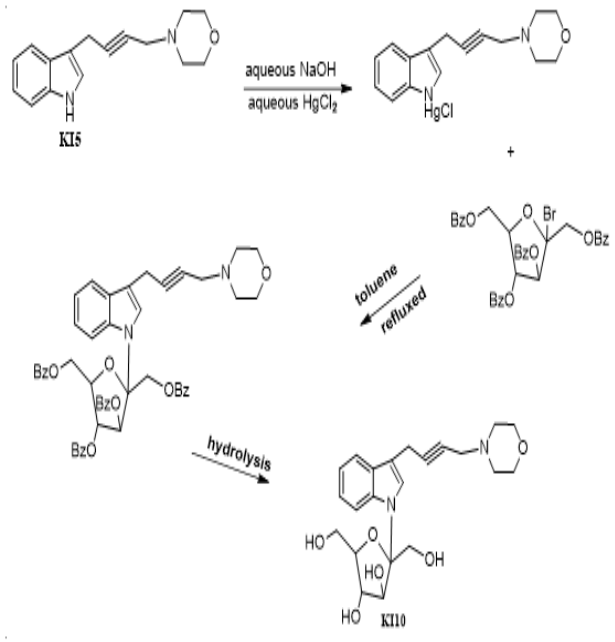

Scheme 4 illustrated stages synthesis of compound KI10

Identification of semi nucleosides derived from indole KI10

Derivative KI10 was prepared by the reaction between KI5, after activating the target site by reacting with mercury chloride in the presence of a strong base to form (a good leaving group) and the product is reacted with a sugar molecule that has been protected with benzoyl chloride [17] and hydrogen bromide, Al-Iraqi et al. [24] then hydrolysis is performed to obtain the required nucleoside. The ratio was 1:1:1 for each one of them. The general equation of preparation appears in scheme 4.

The synthesized derivative KI10 was characterized by measuring melting points, color change, TLC, FT-IR, and 1H-NMR technique. The spectrum IR for compound KI10 in table (5) showed tow stretch band at (2544.19,2665.71Cm-1) for OH, bands absorption disappeared at (3400Cm-1) for NH, bands shifted from (2063Cm-1) to (1967.48Cm-1) for triplet bond C≡C, bands appeared at (3064.99Cm-1) back to CH aromatic, band appeared at(2976.26Cm-1) back to CH aliphatic, bands appeared at (1423.51Cm-1)for C-N, bands shifted from (1618.33Cm-1) to (1683.91Cm-1) for CH aromatic. The spectrum H1NMR for compound (27)KI10 in table (6), showed singlet signal at(δ,2.5ppm) due to six protons of the solvent (DMSO),tow singlet signal at (δ, 3.37ppm),(δ,3.74ppm)for CH2 C10,C13,appeared tow triplet signal at (δ, 2.12ppm) for CH2 C14,C17 and at (δ,3.42ppm)for CH2 C15,C16, the spectrum showed, singlet signal appeared at(δ,4.72 ppm) back to three hydroxyl group in position,C2',C3',C4',C5',doublet signal appeared at (δ,4.9ppm)for OH, group and CH2 in position C6', triplet signal at (δ,3.42ppm)back to CH2 in position C5', singlet signal appeared at(δ,4.72 ppm) back to CH in position C2',C3',C4', singlet signal appeared at (δ, 8.05ppm) back to CH in position C2, triplet signal appeared at (δ, 8.20,8.34ppm) the spectrum showed tow doublet signal at (δ, 7.99 ppm) ,(δ, 8.22 ppm)back to CH in C4 C7 respectively and appearance to singlet signal for hydrogen bond at (δ, 11.04 ppm) and at (δ, 13.34 ppm). All the values we are corresponding to literatures.

Table (5) shows the FT-IR values for synthesized derivative KI10							
Comp. NO.	**Structure**	**IR υ cm-1 (KBr)**					
		N-H	**C-H Aliph**	**C-H Ar.**	**C=C Ar.**	**C-N**	**Others**
KI10	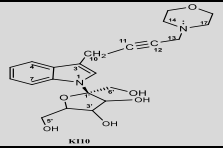 KI10	-----	2976	3064	1683	1423	2544.19,2665.71 OH, 1967 C≡C

Table (6) H1NMR Compound KI10				
Comp. No	**Structure**	**Chemical Shift ppm**	**Type of signal**	**Position of H**
KI10		2.5 6H CH3	S	DMSO
		3.42 4H CH2	t	C15,C16
		2.12 4H CH2	t	C14,C17
		3.37 2H CH2	S	C10
		3.74 2H CH2	S	C13
		4.72 3OH	S	C2',C3',C4'
		4.90 OH	d	C6'
		4.90 2H CH2	d	C6'

	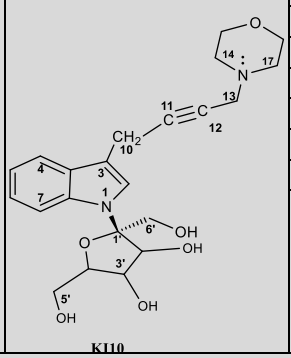 KI10	3.44 1H CH	t	C2',C3',C5'
		8.05 1H CH	t	C2
		7.89 1H CH	d	C4
		8.22 1H CH	d	C7
		8.20 1H CH	t	C5
		8.34 1H CH	t	C6
		11.02 1H	S	H-bond
		13.34 1H	S	H-bond
s = singlet, d=doublet, t= triplet, m= multiplet				

4. Binding with CT-DNA

FT-IR spectra of [KI10]/CT-DNA complex

Indication of [KI10]–DNA complexation comes from the infrared spectroscopic results between 1800 and 600 cm-1 as shown in figure (2). The spectral changes (intensity and shifting) of several prominent DNA-in-plane vibrations at 1649 cm-1 (Gua, 1631 cm-1 (Thy, 1519 cm-1 Ade and1467Cm-1 Cyt), and 1197 cm-1 (PO2 asymmetric stretch) and 1037 cm-1 [25] were monitored at different A–DNA molar ratios.

i) Base binding

In the [KI10]/CT-DNA complexes by decreasing concentration of compound [KI10] (r = 1/100-1/5), observed that the band of Thy was disappeared at all the deferent concentration, the intensity of Gua,, Ade, and Cyt bands increased and reached a maximum at r = 1/5 for Ade, at r = 1/10 for Ade, Cyt and Gua (figure (2). The observed intensity changes can be related to [KI10] interaction with Gua–Cyt and Ade base pairs. At r = 1/5, shifting for the bands at 1649 (Gua) to 1656, 1631 (Thy) disappeared, 1519 (Ade) to 1435, 1467 (Cyt) to 1410 was observed.

The observed shifting was accompanied by increase in intensities of Ade and Cyt bases and phosphate bands that can be attributed to some degree of helix destabilization [22]. As [KI10] concentration increased (r = 1/20-10), shifting for the bands at 1519 (Ade) to 1435, 1467 (Cyt) to 1410 and Po2 shifted from 1197 to 1315Cm-1 (figures (2) was observed in the spectra of [KI10]–DNA complexes. In addition, a major increase in the intensities of Ade was observed, indicating a major interaction with Ade base (minor groove). This should also be due to the fact that Ade bases interact through two hydrogen bonds while Cyt and Gua bases are stabilized by three hydrogen bonds, which account for the former being more prone to perturbation and interaction by [KI10], It provides a suitable steric for molecular rearrangement and interaction. Indeed, some ligand prefers Ade–Thy regions of B-DNA for binding because of the narrower minor groove in Ade–Thy regions (as compared to Gua–Cyt regions of B-DNA) leads to a snug fit of the flat aromatic [KI10] rings between the walls of the groove; also, the higher negative electrostatic possible, attributable in part to the absence of electropositive ANH2 groups along the floor of the groove and the steric advantage of the absence of those same Gua ANH2 groups permit the drug molecule to sinking into the grove [26]. The major shift of Ade and phosphate group with increase of the intensity could be explained by interaction of ligand with Ade and phosphat. In addition, these experiments demonstrated that [KI10] is a good electron acceptor with high polarization ability and dipole moment values, while Ade and Gua–Cyt base pairs are good electron givers, which are favorable for the aromatic stacking interactions between these two systems [27]. Minor increase in the intensities of Cyt, VsPO2 (symmetrical stretching) at ratios r = 1/100-20 are also indicative of some degree of [KI10] interactions with Gua–Cyt base pairs and phosphate groups. This could be explained by some hydrophobic interaction of ligand with Cyt [28]. At r = 1/10, some reduction in the intensity ratios of the bands at 1656 (Gua), 1435 (Ade), 1410 (Cyt), and 1315 (VsPO2) were observed as compared with r=1/20, 1/50, 1/100 (figure (2-34). These losses of intensity ratios were probably due to aggregation of DNA complexes [29]

The major spectral shifting observed for [KI10] in-plane vibrations, are also characteristic of [KI10] interaction via anion- specific donor site. The [KI10] is in monovalent anion form [30] The infrared bands at 2544-2665, 1967, 1683, 1423, 3064, cm-1, assigned to the free [KI10] in-plane HO, C≡C,C=C, CH-aromatic, C-N and vibrations [31], exhibited major shifting upon CT-DNA complexation (figure (2). r = 1/10). The observed spectral changes point to a major [KI10]/CT-DNA interaction through the [KI10]. Similar behavior was observed in the infrared spectra of the aspirin–DNA and ascorbate–DNA complexes, where drug binding was through anion and OH donor atom.

ii) Phosphate binding

The phosphate asymmetric stretching at 1197 cm-1 and symmetric stretching at 1093 cm-1 in the spectrum of free DNA is shifted to 1315 and 1024 cm-1, respectively, when lower concentration of [KI10] is complexed with DNA (r = 1/5; figure (2). Further shifting toward lower wave number (1315 cm-1 for asymmetric PO2 stretching and 1024 cm-1 for symmetric PO2 stretching) is observed when [KI10] is complexed with DNA at higher concentration (r < 1/5) figure (2).

These results also suggest some weak external interaction of [KI10] with the phosphate backbone upon its interaction with the DNA double helix [32] who in FT-IR studies on DNA–[KI10] interaction observed a shift at 1197– 1315 cm-1 (asymmetric PO2 stretch) but, due to

non-satisfactory resolution, could not determine the specific interacting bases.

iii) CT-DNA conformation

Free CT-DNA show B conformation with infrared marker bands at 1649 cm-1 cm-1 (asymmetric PO2 stretch), 670 cm-1 (sugar-phosphate stretch), and 607 cm-1 (phosphodiester mode). In a B-to-A transition, B DNA marker bands at 844 cm-1 due to phosphodiester mode and at 1656 cm-1 due to Gua shift toward lower frequencies, in addition, the band at 1197 cm-1 due to symmetric phosphate vibrations shifts towards higher frequencies about 1315–cm-1 [33, 34]. When a B to Z transition takes place, the band at 607 cm-1 displaces to ca. 844 cm-1 and the band at 1649 cm-1 appears near 1658 cm-1, whereas the band at 1197 cm-1 shifts toward 1315 cm-1 [29]. The changes observed in the bands at 1649 cm-1 and 1197 cm-1 are not indicative of CT-DNA conformational change. The minor spectral change observed in the deoxyribose region 900–500 cm-1 may be attributed to minor alterations in the sugar-phosphate geometry while DNA remains in B state of conformation.

UV-Visible

UV spectra of calf-thymus DNA with varying concentrations of [KI10]. There are four major bands in the spectra for pure DNA, 215 nm (negative), 207 nm (positive), 235 nm (negative), 265 nm (negative) and 274 nm (positive). These are marker UV bands of double helical DNA in B-conformation [22, 35, 36]. When B-to-A DNA transition occurs, UV band at 215 nm becomes less intense, band at 207 nm shifts toward higher wavelength, and band at 274 nm becomes more intense [19, 37, 38]. Binding of [KI10] with CT-DNA does not cause any appreciable shifting in these marker UV bands, indicative of no alteration in B-DNA conformation. This is further confirmed with our infrared spectroscopic results of [KI10,]–DNA interactions, which shows no changes for B-DNA marker bands at 1197cm-1 (PO2) and 844 cm-1 (phosphodiester modes). It should be noted that in a B-to-A transition, these B-DNA marker bands shift from 1197 to 1315 cm-1 (PO2) and 670 to 704 cm-1 (phosphodiester) [39-41]. We did observe these spectral shifting in IR spectra.

The reduction in the intensity of band In the UV spectra at 274 nm is observed for high [KI10] concentrations (r = 1/10 and 1/5). This change may be attributed to CT-DNA aggregation as [KI10] content increases in CT-DNA/drug complexes [38, 42].

The graph in figures (3) and table (7) for the UV rays of the free and complex DNA, where the binding constant K is calculated by calculating the cross-slope ratios shown in the table (8).

Table (7) UV-Visible Absorbance values of the compound (KI10) at different concentrations

1/C KI 10	0.29	0.699	1.4	2.915	5.88
1/ A-A0	0.7	1.4	2.4	0.33	0.827

Table (8) spectrum UV-Visible of free DNA, [KI10]-DNA

Free DNA and DNA derivatives	Absorption A	Binding constant K	Type of transition
Free DNA	0.036	----------	
DNA+ KI10	0.097	1.53	Hyper shift

Bioactive for compounds KI10

In this research, I thought shed light on the biological activity by relying on the inhibition zone of KI10 derivative that were prepared from indole against gram-positive (S. aureus), Staphylococcus aureus is a gram-positive facultative aerobe and a major human pathogen, gram-negative bacteria (E.coli) Escherichia coli is, paradoxically, both the most frequent commensal aero-anaerobic Gram-negative bacillus of the vertebrate gut and one of the main pathogens, being responsible for both intraintestinal and extraintestinal infections [43]. And fungi (Candidate albicans) Candida albicans is normally a harmless commensal of human beings, but it can cause superficial infections of the mucosa (oral/vaginal thrush) in healthy individuals and (rarely) infections of the skin or nails [44]. Where it was distinguished that the compound (KI10) has resistance or an inhibition zone against gram-negative bacteria (E.coli) is higher than the inhibition zone against fungi (Candidate albicans). While there is no inhibition against gram-positive (S. aureus) this we can see clearly through the table (9) and figure (4).

Table (9) inhibition zone for compound KI10

KI10	E.coli	S. aureus	Candidate albicans
Cont.	0	0	0
100%	27	0	12

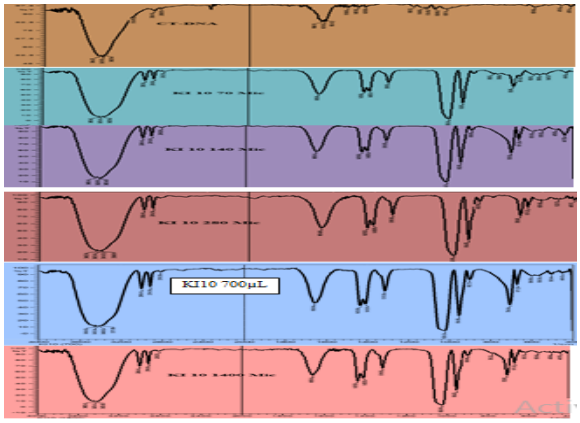

Figure (2) FT-IR spectra of free CT-DNA and [KI10]/CT-DNA complex

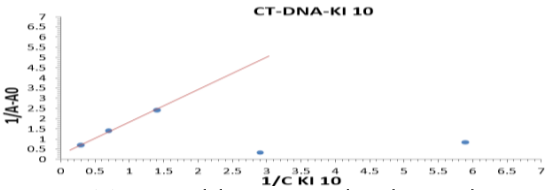

Figure (3) UV-Visible CT-DNA binding with compound KI 10

A0 = the initial absorbance of free DNA nucleic acid

A = the absorbance with different concentration of KI10 at 265 nm

CKI10 = concentration of compound KI10 in solution

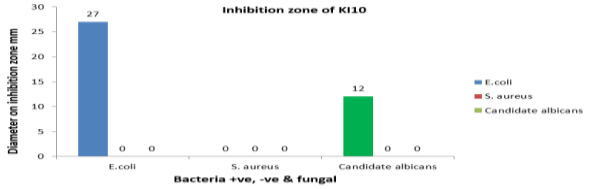

Figure (4) Bioactive compound KI 10 against bacteria +ve,-ve and fungal

References

1. Cordell GA, Quinn-Beattie ML, Farnsworth NR. The potential of alkaloids in drug discovery. Phytotherapy Research: An International Journal Devoted to Pharmacological and Toxicological Evaluation of Natural Product Derivatives. 2001;15(3):183-205. https://doi.org/10.1002/ptr.890

2. Pahari N, Saha D, Jain VK, Jain B, Mridha D. Synthesis and evaluation of acute toxicity studies and analgesic characters of some novel indole derivatives. Int J Pharma Sci Res. 2010;1:399-408. Available from: ijpsr.info/docs/IJPSR10-01-09-13.pdf

3. Rajak H, Veerasamy R, Gupta AK, Kharya MD, Mishra P. Synthesis and Pharmacological Evaluation of New Indolyl-oxadiazoles as anticonvulsant agents. International Journal of Pharmaceutical Sciences and Nanotechnology. 2009;2(3):661-6. https://doi.org/10.37285/ijpsn.2009.2.3.10

4. Medvedev A, Ivanov AS, Veselovsky A, Skvortsov VS, Archakov AI. QSAR analysis of indole analogues as monoamine oxidase inhibitors. Journal of chemical information and computer sciences. 1996;36(4):664-71. https://doi.org/10.1021/ci950126t

5. Seley-Radtke KL, Yates MK. The evolution of nucleoside analogue antivirals: A review for chemists and non-chemists. Part 1: Early structural modifications to the nucleoside scaffold. Antiviral research. 2018;154:66-86. https://doi.org/10.1016/j.antiviral.2018.04.004

6. Yates MK, Seley-Radtke KL. The evolution of antiviral nucleoside analogues: A review for chemists and non-chemists. Part II: Complex modifications to the nucleoside scaffold. Antiviral research. 2019;162:5-21. https://doi.org/10.1016/j.antiviral.2018.11.016

7. Heib A, Niro G, Weck SC, Koppermann S, Ducho C. Muraymycin nucleoside antibiotics: Structure-activity relationship for variations in the nucleoside unit. Molecules. 2019;25(1):22. https://doi.org/10.3390/molecules25010022

8. Peters HL, Jochmans D, De Wilde AH, Posthuma CC, Snijder EJ, Neyts J, Seley-Radtke KL. Design, synthesis and evaluation of a series of acyclic fleximer nucleoside analogues with anti-coronavirus activity. Bioorganic & medicinal chemistry letters. 2015;25(15):2923-6. https://doi.org/10.1016/j.bmcl.2015.05.039

9. Yates MK, Raje MR, Chatterjee P, Spiropoulou CF, Bavari S, Flint M, Soloveva V, Seley-Radtke KL. Flex-nucleoside analogues–novel therapeutics against filoviruses. Bioorganic & medicinal chemistry letters. 2017;27(12):2800-2. https://doi.org/10.1016/j.bmcl.2017.04.069

10. Wani TA, Alsaif N, Bakheit AH, Zargar S, Al-Mehizia AA, Khan AA. Interaction of an abiraterone with calf thymus DNA: Investigation with spectroscopic technique and modelling studies. Bioorganic Chemistry. 2020;100:103957. https://doi.org/10.1016/j.bioorg.2020.103957

11. Shahabadi N, Maghsudi M. Multi-spectroscopic and molecular modeling studies on the interaction of antihypertensive drug; methyldopa with calf thymus DNA. Molecular biosystems. 2014;10(2):338-47. https://doi.org/10.1039/C3MB70340A

12. Pan M-H, Ho C-T. Chemopreventive effects of natural dietary compounds on cancer development. Chemical Society Reviews. 2008;37(11):2558-74. https://doi.org/10.1039/B801558A

13. Sobha S, Mahalakshmi R, Raman N. Studies on DNA binding behaviour of biologically active transition metal complexes of new tetradentate N2O2 donor Schiff bases: Inhibitory activity against bacteria. Spectrochimica Acta Part A: Molecular and Biomolecular Spectroscopy. 2012;92:175-83. https://doi.org/10.1016/j.saa.2012.02.063

14. Erkkila KE, Odom DT, Barton JK. Recognition and reaction of metallointercalators with DNA. Chemical Reviews. 1999;99(9):2777-96. Available from: https://resolver.caltech.edu/CaltechAUTHORS:20160407-115524676

15. Barone G, Terenzi A, Lauria A, Almerico AM, Leal JM, Busto N, Garcia B. DNA-binding of nickel (II), copper (II) and zinc (II) complexes: Structure–affinity relationships. Coordination Chemistry Reviews. 2013;257(19-20):2848-62. https://doi.org/10.1016/j.ccr.2013.02.023

16. Berman HM, Westbrook J, Feng Z, Gilliland G, Bhat TN, Weissig H, Shindyalov IN, Bourne PE. The protein data bank. Nucleic acids research. 2000;28(1):235-42. https://doi.org/10.1093/nar/28.1.235

17. Yu RT, Friedman RK, Rovis T. Enantioselective rhodium-catalyzed [4+ 2+ 2] cycloaddition of dienyl isocyanates for the synthesis of bicyclic azocine rings. Journal of the American Chemical Society. 2009;131(37):13250-1. https://doi.org/10.1021/ja906641d

18. Minvielle MJ. Controlling Bacterial Pathogenic Behaviors using Indole-containing Small Molecules. 2014. Available from: file:///C:/Users/MUHAMMAD%20ALI/Downloads/etd.pdf

19. Al-Araji SM, Ali RA. Synthesis of new Mannich bases from indole derivatives. Baghdad Science Journal. 2012;9(1).

20. Fattah MY, Al-Ani MM, Al-Lamy MT. Studying collapse potential of gypseous soil treated by grouting. Soils and Foundations. 2014;54(3):396-404. https://doi.org/10.1016/j.sandf.2014.04.008

21. Vijayalakshmi R, Kanthimathi M, Subramanian V, Nair BU. DNA cleavage by a chromium (III) complex. Biochemical and biophysical research communications. 2000;271(3):731-4. https://doi.org/10.1006/bbrc.2000.2707

22. Saito ST, Silva G, Pungartnik C, Brendel M. Study of DNA–emodin interaction by FTIR and UV–vis spectroscopy. Journal of Photochemistry and Photobiology B: Biology. 2012;111:59-63. https://doi.org/10.1016/j.jphotobiol.2012.03.012

23. Snyder H, Smith CW, Stewart JM. Carbon-alkylation with quaternary ammonium salts. A new approach to the synthesis of compounds containing the β-indolemethylene

group. Journal of the American Chemical Society. 1944;66(2):200-4. https://doi.org/10.1021/ja01230a012
24. Al-Iraqi MA, Yahya AM. Synthesis of some N-Aryl-p-Toluene Sulfonamide Compounds. Rafidain journal of science. 2009;20(4E). Available from: http://www.pdffactory.com/
25. Jangir DK, Charak S, Mehrotra R, Kundu S. FTIR and circular dichroism spectroscopic study of interaction of 5-fluorouracil with DNA. Journal of Photochemistry and Photobiology B: Biology. 2011;105(2):143-8. https://doi.org/10.1016/j.jphotobiol.2011.08.003
26. Reddy BP, Sondhi SM, Lown JW. Synthetic DNA minor groove-binding drugs. Pharmacology & therapeutics. 1999;84(1):1-111. https://doi.org/10.1016/S0163-7258(99)00021-2
27. Riahi S, Eynollahi S, Ganjali MR. Interaction of emodin with DNA bases: a density functional theory. Journal of Theoretical and Computational Chemistry. 2010;9(05):875-88. https://doi.org/10.1142/S0219633610006055
28. Biological ISf, Repositories E. Collection, storage, retrieval and distribution of biological materials for research. Cell Preservation Technology. 2008;6(1):3-58. https://doi.org/10.1089/cpt.2008.9997
29. Jangir DK, Tyagi G, Mehrotra R, Kundu S. Carboplatin interaction with calf-thymus DNA: A FTIR spectroscopic approach. Journal of Molecular Structure. 2010;969(1-3):126-9.
30. Wang D, Yang G, Song X. Determination of pKa values of anthraquinone compounds by capillary electrophoresis. Electrophoresis. 2001;22(3):464-9. https://doi.org/10.1002/1522-2683(200102)22:3%3C464::AID-ELPS464%3E3.0.CO;2-4
31. Harry-O'kuru RE, Wu YV, Evangelista R, Vaughn SF, Rayford W, Wilson RF. Sicklepod (Senna obtusifolia) seed processing and potential utilization. Journal of agricultural and food chemistry. 2005;53(12):4784-7. https://doi.org/10.1021/jf040483g
32. Bi S, Zhang H, Qiao C, Sun Y, Liu C. Studies of interaction of emodin and DNA in the presence of ethidium bromide by spectroscopic method. Spectrochimica Acta Part A: Molecular and Biomolecular Spectroscopy. 2008;69(1):123-9. https://doi.org/10.1016/j.saa.2007.03.017
33. Nafisi S, Norouzi Z. A comparative study on the interaction of cis-and trans-platin with DNA and RNA. DNA and Cell Biology. 2009;28(9):469-77. https://doi.org/10.1089/dna.2009.0894
34. Nafisi S, Kahangi FG, Azizi E, Zebarjad N, Tajmir-Riahi H-A. Interaction of zanamivir with DNA and RNA: Models for drug–DNA and drug–RNA bindings. Journal of molecular structure. 2007;830(1-3):182-7. https://doi.org/10.1016/j.molstruc.2006.09.032
35. Vorlíčková M, Kejnovská I, Bednářová K, Renčiuk D, Kypr J. Circular dichroism spectroscopy of DNA: from duplexes to quadruplexes. Chirality. 2012;24(9):691-8. https://doi.org/10.1002/chir.22064
36. Xiao Y, Xu K, Wang Q, Xiong X, Huang Y, Li H. Synthesis, structure, and calf-thymus DNA binding of ternary fleroxacin–Cu (II) complexes. RSC Advances. 2016;6(83):80286-95. https://doi.org/10.1039/C6RA18971G
37. Subastri A, Ramamurthy C, Suyavaran A, Rao PL, Babu EP, Krishna KH, Kumar MS, Thirunavukkarasu C. Probing the interaction of troxerutin with transfer RNA by spectroscopic and molecular modeling. Journal of Photochemistry and Photobiology B: Biology. 2015;153:137-44. https://doi.org/10.1016/j.jphotobiol.2015.09.013
38. Al-doury S, Al-Nasrawi M, AL-Samarraie M. The molecular sequence of Giardia lamblia by using (tpiA) and (tpiB). International Journal of Drug Delivery Technology. 2019;9(03):374-7.
39. CN N. soukpoe-Kossi, AA Ouameur, T. Thomas, A. Shirahata, TJ Thomas and HA Tajmir-Riahi. Biomacromolecules. 2008;9:2712-8.
40. AL-Samarraie MQ, Omar MK, Yaseen AH, Mahmood MI. The wide spread of the gene haeomolysin (Hly) and the adhesion factor (Sfa) in the E. coli isolated from UTI. Journal of Pharmaceutical Sciences and Research. 2019;11(4):1298-303.
41. AL-Samarraie MQ, Yaseen[1] AH, Ibrahim BM. MOLECULAR STUDY OF POLYMORPHISM FOR GENE TNF-ALPHA USING ARMS-PCR TECHNIQUE FOR PATIENTS WITH RHEUMATOID ARTHRITIS. Biochem Cell Arch Vol. 2019;19:4285-90. Https://doi.org/10.35124/bca.2019.19.2.4285
42. Abderrezak A, Bourassa P, Mandeville J-S, Sedaghat-Herati R, Tajmir-Riahi H-A. Dendrimers bind antioxidant polyphenols and cisplatin drug. PloS one. 2012;7(3):e33102. https://doi.org/10.1371/journal.pone.0033102
43. Tenaillon O, Skurnik D, Picard B, Denamur E. The population genetics of commensal Escherichia coli. Nature reviews microbiology. 2010;8(3):207-17. https://doi.org/10.1038/nrmicro2298
44. Gow NA, Yadav B. Microbe Profile: Candida albicans: a shape-changing, opportunistic pathogenic fungus of humans. Microbiology. 2017;163(8):1145-7. https://doi.org/10.1099/mic.0.000499